JAKU: Earth Sci., **Vol. 21,** No. 1, pp: 1-25 (2010 A.D. / 1431 A.H.)
DOI: 10.4197 / Ear. 21-1.1

Integration of Geologic and Remote Sensing Studies for the Discovery of Uranium Mineralization in Some Granite Plutons, Eastern Desert, Egypt

M.H. Shalaby, A.Z. Bishta*, M.E. Roz and **M.A. El Zalaky**
Nuclear Materials Authority, Cairo, Egypt
**Faculty of Earth Sciences, King Abdulaziz University, Jeddah, Saudi Arabia*
abishta@kau.edu.sa

Received: 29/10/2008 Accepted: 8/6/2009

Abstract. The main objective of this research is to integrate geology with remote sensing techniques to establish common characteristic features leading to the recognition of other uranium mineralizations within the Pan-African younger granites of the Eastern Desert of Egypt. The association of aplites, quartz and jasperoid veins and lamprophyric dykes as well as alteration processes throughout and near the mineralized sectors appear to play an important role in the distribution and localization of the mineralization.

Image processing techniques were applied on the digital subset ETM+ data covered the studied areas. These techniques generated several products of enhanced satellite imagery, such as colour composite images, ratio images and principal component images. These techniques have been successfully used in the lithological discrimination of uranium-bearing granites. The capabilities of remote sensing data to characterize the uranium bearing granites, in addition to characterization and mapping the hydrothermal alteration zones usually helps in localization of uranium mineralizations. Extensive field geologic and radiometric investigations to the pronounced zones delineated by the image processing technique, led to discovery of four locations of high radioactive anomalies with some uranium mineralizations, mainly connected to the studied younger granites.

Mineralogical studies were carried out, using ore and scanning microscope and XRD, for some selected mineralized samples. These

investigations confirm the presence of uranophane mineral as uranyl silicates. The uranophane mineral is found in close association with hematite, quartz, calcite and chlorite. Relics of corroded pyrite grains are disseminated in the groundmass and filling some vugs and cavities. The uranium mineralization is found adsorbed and enclosed around pyrite. This may indicate that the presence of pyrite created a reduced environment favourable for the precipitation and fixation of uranium.

Introduction

The granitic rocks are considered as one of the most important source for uranium deposits. Comprehensive exploration programs are conducted by the Nuclear Materials Authority (NMA) to search for uranium deposits in Egypt. These programs led to discovery of radioactive anomalies and uranium mineralizations in the Northern, Central and Southern Eastern Desert of Egypt. The present work concerns with Gabal (G) Gattar, G. El Missikat and G. El Erediya uranium prospects (Fig. 1) as well as they represent the most promising prospects for uranium mineralizations.

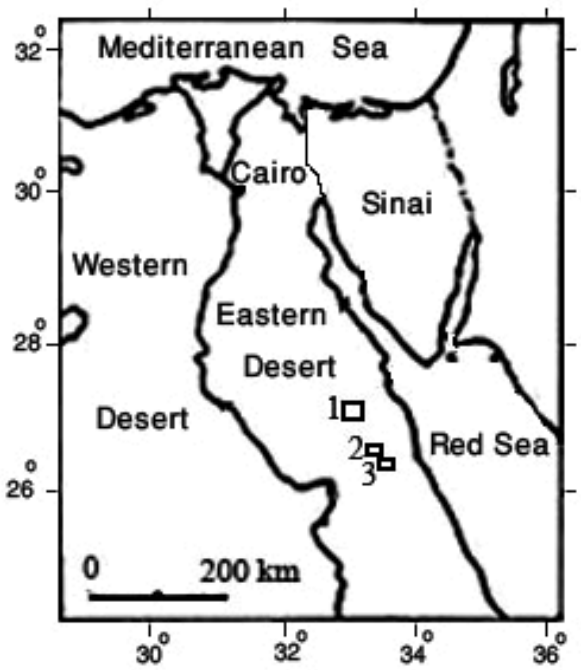

Fig. 1. Location map of the studied areas, 1- G. Gattar, 2- G. El Missikat, 3- G. El Erediya.

Image Processing techniques were applied in this work to define the main characteristic features of the granitic rock-bearing uranium mineralizations. The enhanced thematic mapper plus (ETM+) digital data of Landsat 7 satellite was used to recognize and map the investigated areas. The constructed colour composite images and application of principal component analyses of ETM+ data led to identify and characterize the uranium-bearing granites in the investigated areas.

Geology

Gabal Gattar, G. El Missikat and G. El Erediya areas, as a part of the Eastern Desert of Egypt, have been subjected to many geological studies and activities related to the exploration of economic mineral deposits. The granitic rocks of the study areas are leucocratic, highly differentiated with the presence of zircon, monazite, fluorite, iron oxides, and apatite as accessories (Roz, 1994, El Kassas, 1974 and Bakhit, 1978). El Kassas (1974) found that the majority of the radioactive anomalies and the uranium occurrences in El Erediya pluton are connected and associated with the aplite dykes and jasperoid veins intruded through pink granites. Nossair (2005) achieved a comparative structural study of both surface and subsurface at G. Gattar pluton. He concluded that the predominant joint and fracture trends recorded at the topographic surface are still persistent and nearly possess the same intensities at the subsurface, escorted with the same types of alteration features.

Geochemically, the granitic rocks of the study areas are characterized by high silica contents (more than 73%), metalumonous to slightly peralumonous, low Fe_2O_3, MgO and TiO_2, rich in alkali elements (Na_2O and K_2O), low Th/U ratio, and low $^{87}Sr/^{86}Sr$. They also are rich in trace elements such as Nb, Ga, Zr, Y, U and Th (El Sayed *et al.*, 2003, Ibrahim, 2002 and Abdalla and El Afandy, 2004). In the granitic magma of metaulminous nature, the largest amount of uranium contents are bound to the structure of the accessory minerals, especially zircon, that contain abnormally high value of U, ranging from about 3000 to 11000 ppm (Abou Deif, 1992). This uranium can be easily mobilized and leached only after metamictization, at least 100 Ma after the emplacement of the granite (Cuney, 1999).

The uranium mineralizations associated with the studied granites occurred after granite crystallization (at least about 100-200 Ma) as indicated by 420 Ma time gap between the emplacement of El Erediya younger granite (583 Ma) and deposition of primary uranium minerals (160 Ma) (Abou Deif, 1992). The association of aplites, silica and jasperoid veins and lamprophyric dykes around and near the mineralized sectors appear to play an important role in the mineralization processes. They act as heat source causing increase of the mobility of the uranium and its leachability. The tectonic and geochemical characteristics of the studied granites indicated that their magmas originated in post orogenic and within-plate tectonic environment (Greenberg, 1981 and Attawyia, 1990). Some few works dealing with the image processing techniques and geological interpretations using satellite images for the study areas had been achieved (El Rakaiby and Shalaby, 1992, El Rakaiby, 1995, El Rakaiby 1997, Bishta, 2004 and Mostafa and Bishta, 2005).

Image Processing of Remotely Sensed Data

The remotely sensed raw data of the studied areas are included in Landsat-7 Enhanced Thematic Mapper Plus (ETM+) data scenes number 175/41 (Path/Row) covers G. Gattar area and 174/42 covers G. El Missikat and G. El Erediya areas. Subsets of the digital ETM+ imagery covering the studied areas were obtained. The image processing techniques were applied in this work using ENVI 3.4 and PCI, GeoAnalyst software-package. Geometric correction has been done for the digital data of the ETM+ bands of the study areas. Raw digital satellite data usually includes geometric distortions due to sensor geometry, scanner, platform instabilities, earth rotation, earth curvature, *etc*. and it is necessary to correct and adapt them (Mather, 1987, Lillesand *et al.*, 2004, Richards, 1995). The georeferencing is carried out using ground control points selected from topographic sheets of scale 1:50,000.The root mean square error (RMS) in the geometric processing was 0.54 (Bernstein, 1978). The following parameters have been used in the registration procedures: UTM Projection, Zone 36N, Row 42 and Datum Egypt.

Image enhancement techniques were applied to the selected subset of the ETM+ data for the two study areas of Gattar pluton and El Missikat and El Erediya plutons. The achievement of the goal of the

application of remote sensing techniques on the studied granites led to identify and characterize the studied uranium-bearing granites based on the different remote sensing processes of ETM+ data such as color composite image, principal component and band ratio images.

1- Colour Composite Images of ETM Data

Digital images are typically displayed as additive colour composites using the three primary colours, red, green and blue (RGB). Different spectral bands of ETM+ data have been selected and combined in RGB colour system to make colour composite images for the studied areas. These combinations were tried to select the best colour composite ETM image to be useful in extracting meaningful information about visual lithological discrimination of the studied granitic rocks such as combination of ETM bands 7, 4 and 2 (Fig.2).

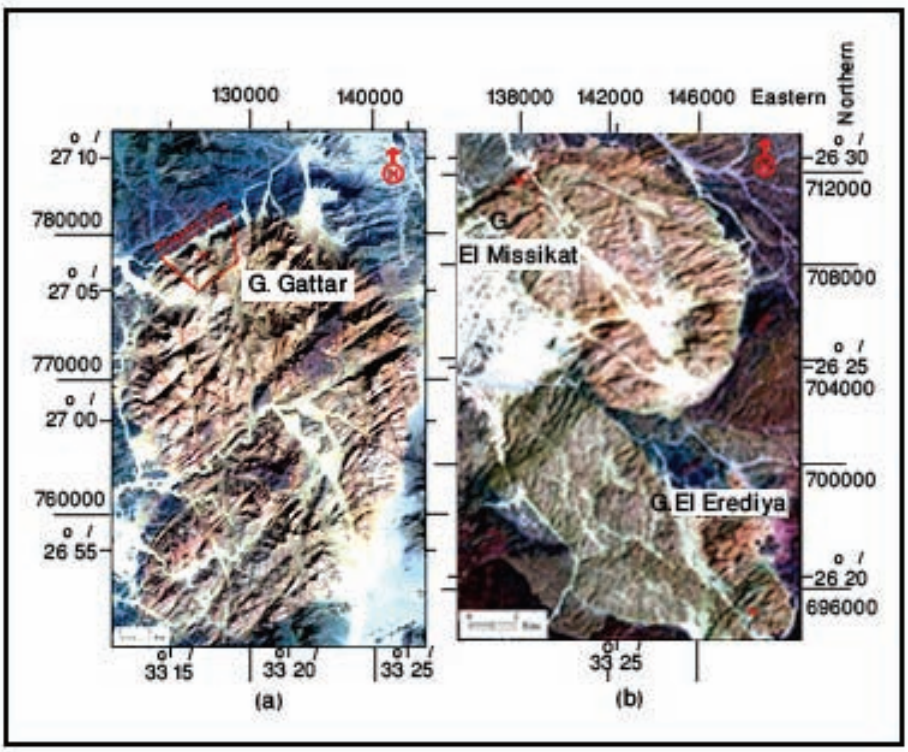

Fig. 2. False colour composite ETM image of: (a) Gattar pluton, and (b) El Missikat and El Erediya areas (Bands 7, 4, 2 displayed in RGB).

2- Principal Component Analysis of ETM+ Data

Different bands of multispectral data are often correlated and thus contain similar information *i.e*. have similar visual appearances. This correlation means that there is redundancy of information. The principal components (PC) transformation is used, to reduce this data redundancy, by compressing multispectral data sets and calculating a new coordinate system (Sabins, 1999). The application of the PC on the present data is to compress all of the information contained in an original n-channel (band) data set, into fewer number of channels or components, that could be displayed separately as single stretched PC-images, or as component in color composite PC-image (Vincent, 1997). The colour composite image of principal components PC1, PC2 and PC3 for the studied areas successfully distinguish and characterize the studied granites of Gattar, El Missikat and El Erediya granites (Fig. 3).

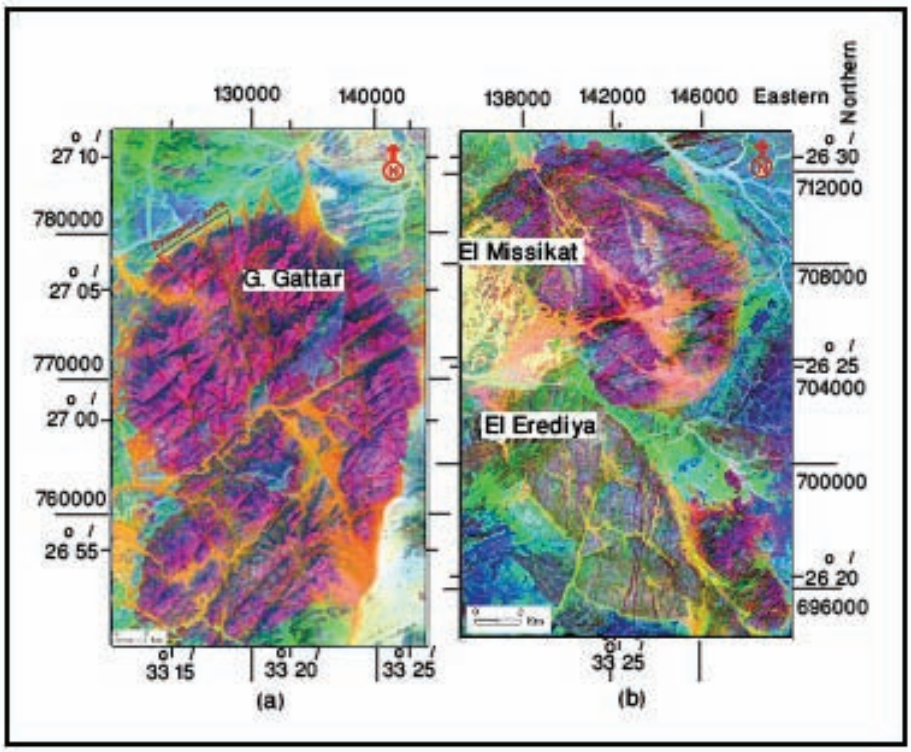

Fig. 3. False colour composite ETM+ images of principal components PC1, PC2, PC3 displayed in RGB for: (a) Gattar pluton, and (b) Missikat and El Erediya area.

3- Band Ratios of ETM+ Data

Addition, subtraction, multiplication and division of the pixel brightness from two bands of image data to form a new image are particularly simple transformations to apply in image processing technique. Multiplication seems not to be as useful as the others, band differences and ratios being most common. Differences can be used to highlight regions of change between two images of the same area. Ratios of different spectral bands from the same image are found useful in reducing the effect of topography and for enhancing subtle differences in the spectral reflectance characteristics for rocks and soils (Richards, 1995). The use of the band ratio technique was applied to the satellite ETM+ Landsat 7 digital data for the study areas. Figures 4 (a & b) show examples of ETM band ratio 5/7 images for G. Gattar pluton and El Erediya and El Misikat areas respectively. Figures 4 (c & d) are band ratio 3/1 images for G. Gattar pluton and El Erediya and El Misikat areas respectively. Sultan *et al*. (1986, 1987) used band ratios of the digital data of Landsat thematic mapper for lithologic mapping in the Eastern Desert of Egypt. They used ratios of TM bands 5/1, 5/7 and 5/4X3/4 for constructing a colour composite image. These band ratios were applied for constructing a colour composite image of the study area as shown in Fig. 4 (c).

The reflectance values in band 7 (2.08 to 2.35 μm) of TM data depend mainly on the hydroxyl content of the rocks. The ratio of band 5 to band 7 was used as a measure of the intensity of the hydroxyl absorption (2.2 to 2.4 μm region). This ratio was used because band 5 is not within the confines of the Fe –bearing aluminosilicate related or hydroxyl-related absorption features, whereas band 7 is within the hydroxyl absorption wave lengths (Sultan *et al.* 1987). The high value of band 5/7 ratio appears in light tone due to the high content of hydroxyl-bearing minerals (characterizing the metavolcanics and Dokhan volcanics). The younger granitic rocks are poor in hydroxyl bearing minerals and opaques so they show lower band 5/7 ratio and appear in dark tone (Fig. 4 a & b).

The spectral band ratio is one of the most common powerful techniques applied for mapping the minerals of alteration zones (clay,

alunite and iron minerals) (Sabins, 1999). Recognition of hydrothermal altered rocks associated with mineral deposits was carried out using image processing techniques such as band ratio images in addition to colour ratio composite images. The spectral bands of ETM+ are well-suited for recognizing assemblage of altered minerals. The hydrothermal minerals that were detected by the Landsat image processing of the data of selected areas could be classified into two groups: hydroxyl (clay minerals) and hydrated mineral (alunite and jarosite) detected by band ratio 5/7 (Fig. 4 a & b) on one hand, and minerals containing iron (hematite and goethite,) detected by band ratio 3/1 on the other hand (Fig. 4 c & d). Appling these techniques led to the recognition of more than fifteen zones of altered rocks within the studied granites.

4- Colour Composite ETM+ Band Ratio Images

Colour composite images have been constructed using combination of three ETM band ratios. Different ETM band ratio combinations were carried out to select the optimum colour composite image to use in the visual lithologic discrimination of the investigated area. Some of these combinations are illustrated in (Fig. 5). The best selected result was the colour composite image produced by the combination of bands 5/7, 4/5 and 5/1 (Fig. 5).

This selected image was prepared (scale 1 : 100,000) as shown in (Fig. 5) in which band 5/7 image was assigned by the red component, band 4/5 image by the green component and band 5/1 image by the blue component. The selected colour composite image (Fig. 5) diagnoses some aspects between the different rock units, which was not obviously identified in the FCC image in (Fig. 3). For example, it determines and delineates the intrusions of the youmger granitic rocks (green colour) into the Dokhan volcanics (rose colour), in Gabal Abu Dokhan and Gabal Um Guruf. The younger granitic rocks display green colour in this image (Fig. 5) due to the high band 4/5 ratio. The metavolcanics (mv) appear on this image in blue colour due to the high band 5/1 ratio. The boundaries between the metavolcanics, the younger granites and the older granites could be delineated in the southern part of the mapped area using the colour composite image of ratio bands (Fig. 5).

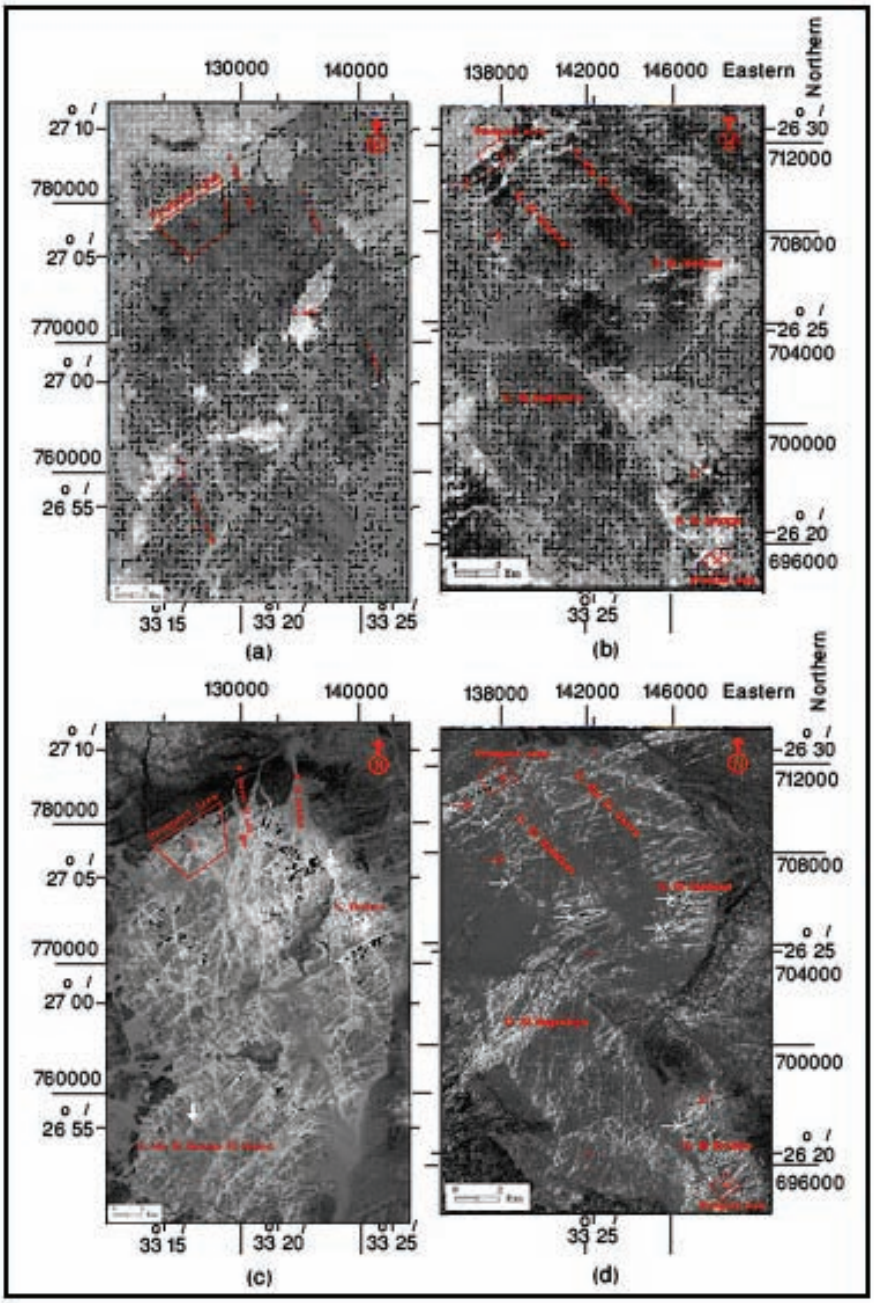

Fig. 4. Landsat ETM band ratio images showing the alteration zones in bright image signature in the study areas : (a) ETM 5/7 ratio of Gattar pluton, (b) ETM 5/7 ratio of El Missikat and El Erediya plutons, (c) ETM 3/1 ratio of Gattar pluton, and (d) ETM 3/1 ratio of El Missikat and El Erediya plutons.

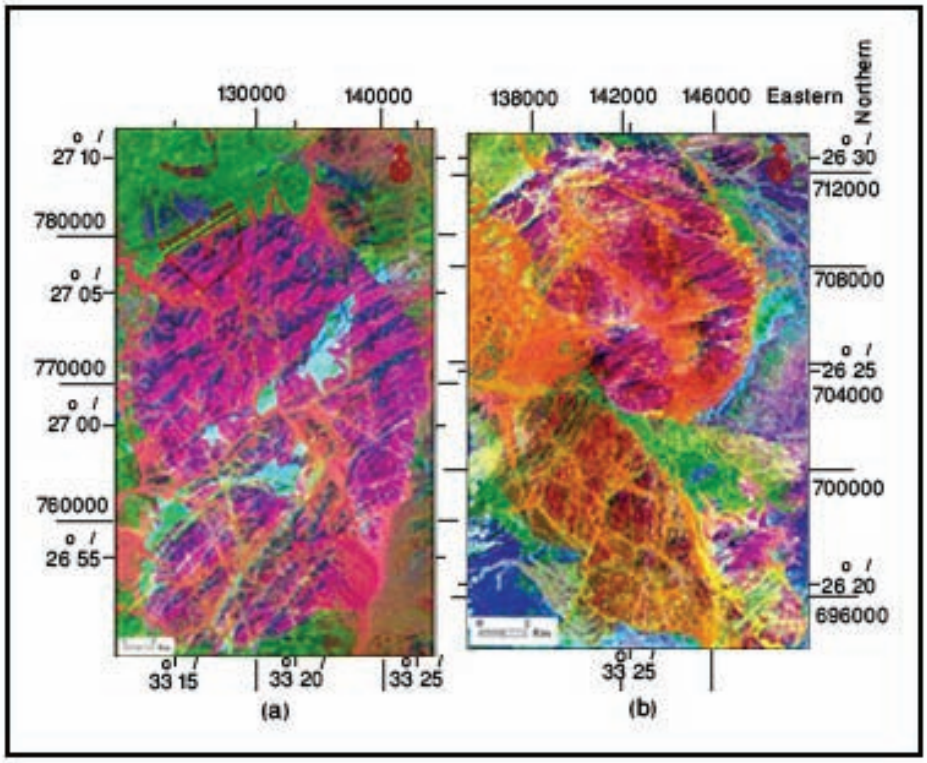

Fig. 5. False colour composite ETM band ratio image of : (a) Gattar pluton, (b) El Missikat and El Erediya plutons.

5- Lineaments Extraction

The automatic lineaments extraction from Landsat ETM+ panchromatic band of the study areas was carried out under the default parameters of GeoAnalyst-PCI package. These lineaments have been visually edited to extract only the structural lineaments. The obtained total structural lineaments for Gattar pluton scored 1456. The rose diagram of these lineaments shows that their predominant trend is NE-SW (Fig. 6). The zones of high lineament intensities concentrated at the extreme northern part of Gattar pluton (prospect area), western part of the pluton (G. Thalma) and at G. Abu El Hassan El Ahmar. The intersected lineaments, on the other hand, are found to be restricted and concentrated only in the northern part of the pluton (prospect area) and in narrow zones of G. Abu El Hassan El Ahmar (Fig. 6).

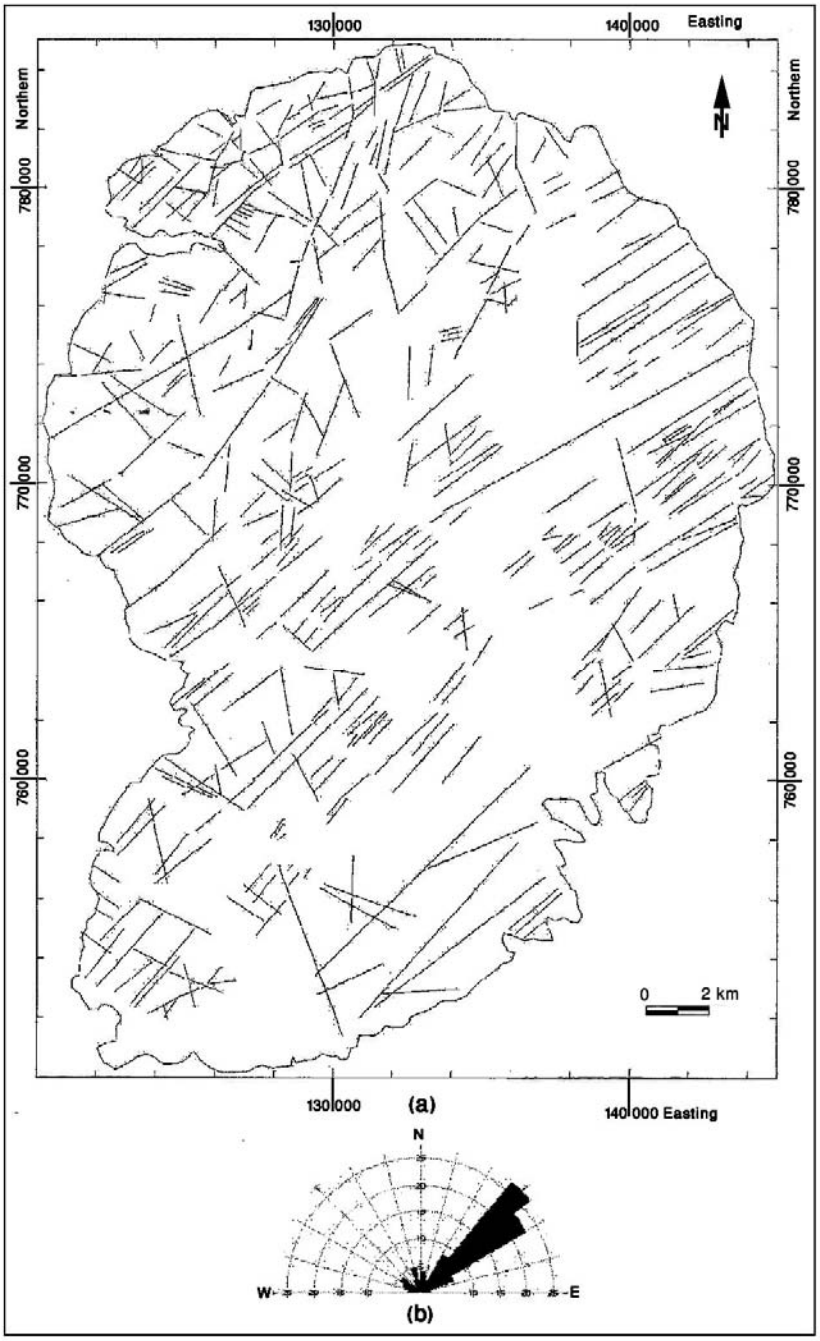

Fig. 6. (a) Structural lineaments extracted from panchromatic ETM image, and (b) their frequency rose diagram for Gattar pluton.

The extracted structural lineaments for El Missikat pluton measured 984 in number. The rose diagram of these structural lineaments indicates that the predominant trends are represented by the ENE-WSW and NE-SW directions (Fig. 7). The northwestern part of El Missikat pluton (West of the prospect area) and the western parts posses the highest lineaments density, while the northwestern and central parts of the pluton are characterised by the oncentration of lineaments intersection.

Regarding El Erediya pluton, the extracted structural lineaments (Fig. 8) measured 331 in number and their rose diagram indicate that the most predominant trend is NE-SW direction. The central and southern part of the pluton posses the highest intensity of lineaments, while the lineaments intersected zones are represented by the southern west and northern parts of El Erediya pluton.

It could be concluded that the alteration zones and/or mineralized zones in the investigated areas, delineated by band ratio images of the studied granites coincide more or less with high lineaments intensity and/or high lineaments intersection or both together.

6- Image Criteria of the Study Areas and the New Discovered Uranium Mineralized Zones

From the previously studied remotely sensed data, it is worth mentioning that there are many criteria of the alteration zones that could be used as a guide for the exploration of uranium mineralization in the Egyptian younger granites. Table 1 lists the most important criteria that can be considered as tools to increase the potentiality of the uranium mineralization. Moreover, construction of the alteration maps of the different studied plutons interpreted from the image processing helped in the discovery of the new zones of mineralization (Fig. 9, 10 & 11) and could be used in the exploration for uranium mineralization in the future.

The methods applied in this work for the exploration of hydrothermal uranium mineralization using satellite image processing, are based on the surface spectral features characteristic of this type of hydrothermal uranium mineralization, that, will allow favourable areas for exploration. The occurrence of hydrothermal altered rock is one of the main features that can be utilized to determine the localization of uranium mineralization. By comparing the intensity of the extracted

structural lineaments, and their intersections to the altered zones, depicted from remote sensing processing technique, it could be recognized that the alteration zones, more or less coincide with the high frequency and intersected lineaments.

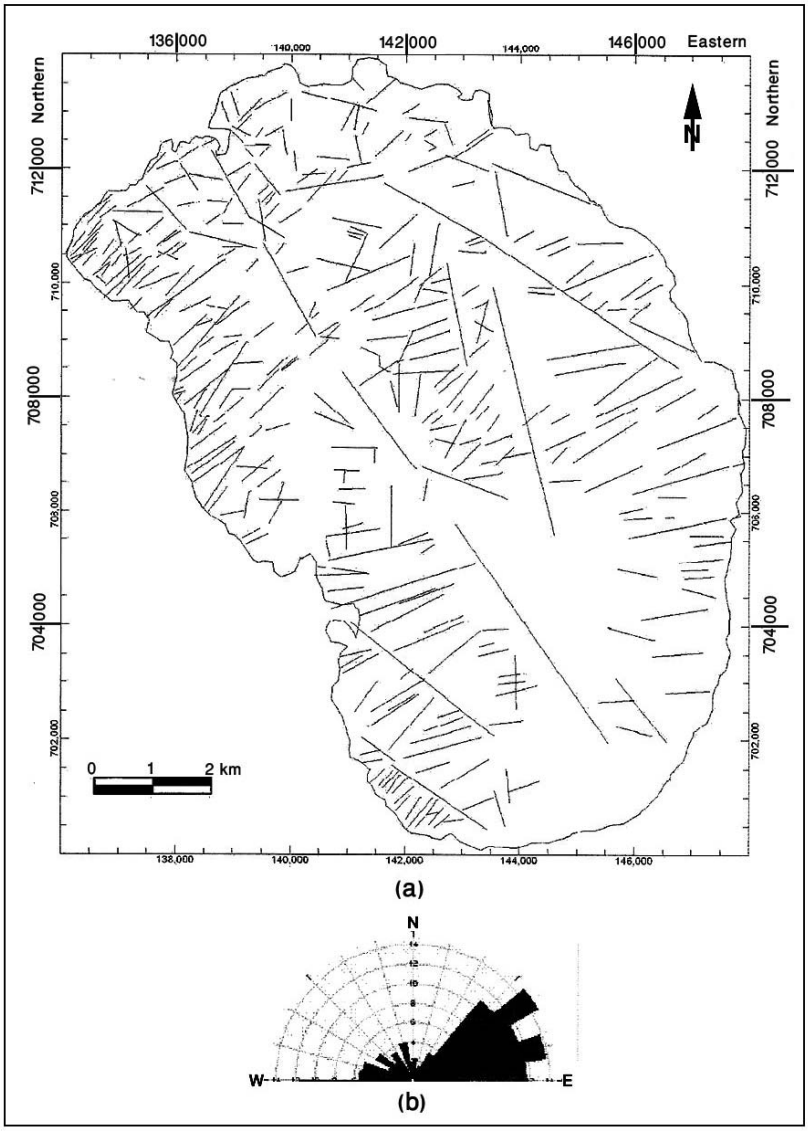

Fig. 7. (a) Structural lineaments extracted from panchromatic ETM image, and (b) their frequency rose diagram for El Missikat pluton.

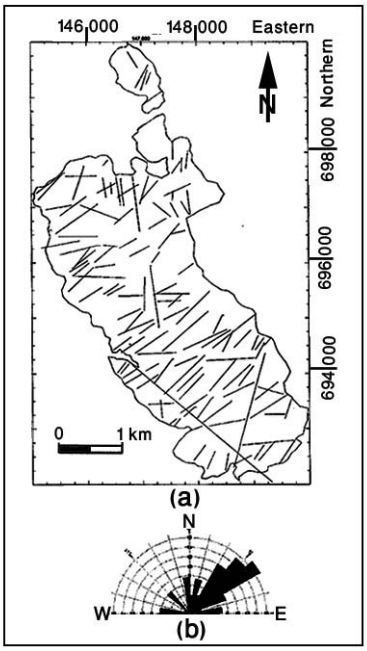

Fig. 8. (a) Structural lineaments extracted from panchromatic ETM image, and (b) their frequency rose diagram for El Erediya pluton.

The distribution of hydrothermal alteration within the processed Landsat images become the key to locate the main outflows of a hydrothermal system, which led, after the field checking, to recognize highly radioactive anomalies and mineralized zones within the study areas. Therefore, many locations are delineated in this work as altered zones, whether by clay minerals, jarosite and alunite or by iron oxides. Iron oxides are frequently observed in the outcrops of hydrothermally altered rocks. Therefore their identification is a useful key to define areas related to deeply mineralized zones (Fig. 9, 10 & 11).

Field Proving with Laboratory Investigations

Extensive geological, field proving and radiometric investigations were carried out for the alteration zones (Fig. 12), delineated in the studied granites by the Landsat image processing. During the field works, the radiometric investigations revealed that the gamma radioactivity of all altered zones is relatively high. The only four locations discovered as high radioactive anomalies with some uranium mineralizations, are mainly connected to the studied younger granites, while the other zones

were not subjected to detailed investigations due to the rugged topography of their host rocks.

Table 1. The image criteria of both prospect areas and new discovered uranium ineralized zones.

Prospect areas previously discovered	New discovered mineralized zones in this study	Image criteria
G. Gattar (G-I, G-II, GV & GVI)		High reflectance to band 3/1 ratio (iron oxide altered minerals) – Low reflectance to band 5/7 ratio (hydroxyl altered minerals) – High lineament frequency and lineament intersection – Yellowish colour in colour composite ratio (CCR)1 of 3/1, 3/2, 5/7
	1- W. Mayet El Abd mineralized zone, North G.Gattar area.	High reflectance to band 3/1 ratio (iron oxide altered minerals) – Low to moderate reflectance to band 5/7 ratio (hydroxyl altered minerals) – Highly lineament frequency and low lineament intersection – Yellowish colour in CCR1 of 3/1, 5/4, 5/7
G. El Missikat		High reflectance to band 5/7 ratio (hydroxyl and hydrated altered minerals) – Low to moderate reflectance to band 3/1 ratio (iron oxides altered minerals) – Moderate to low lineament and lineaments intersection – High reflectance to PC4 – Greenish Yellow colour in CCR1 of 5/1, 5/7, 5/4x3/4
	2- Northwestern mineralized zones of G. El Missikat	Moderate to low reflectance to band 5/7 ratio (hydroxyl altered minerals) – High reflectance to band 3/1 ratio (iron oxides altered minerals) – Higher lineament frequency and low lineaments intersection – High reflectance to PC4 – Yellowish green colour in CCR1 of 5/1, 5/7, 5/4x3/4
	3- Western zone of G. El Missikat	Moderate to low reflectance to band 5/7 ratio (hydroxyl altered minerals) – High reflectance to band 3/1 ratio (iron oxides altered minerals) – Higher lineament frequency and low lineaments intersection – High reflectance to PC4 – Greenish Yellow colour in CCR1 of 5/1, 5/7, 5/4x3/4
G. El Erediya		High reflectance to band 5/7 ratio (hydroxyl altered minerals) – Moderate reflectance to band 3/1 ratio (iron oxides altered minerals) – Higher lineament frequency and low lineaments intersection – High reflectance to PC4 – Greenish Yellow colour in CCR1 of 5/1, 5/7, 5/4x3/4
	4- Northern mineralized zone of G. El Erediya	High reflectance to band 5/7 ratio (hydroxyl and hydrated altered minerals) – High reflectance to band 3/1 ratio (iron oxides altered minerals) – Higher lineament frequency and low lineaments intersection – High reflectance to PC4 – Greenish Yellow colour in CCR1 of 5/1, 5/7, 5/4x3/4

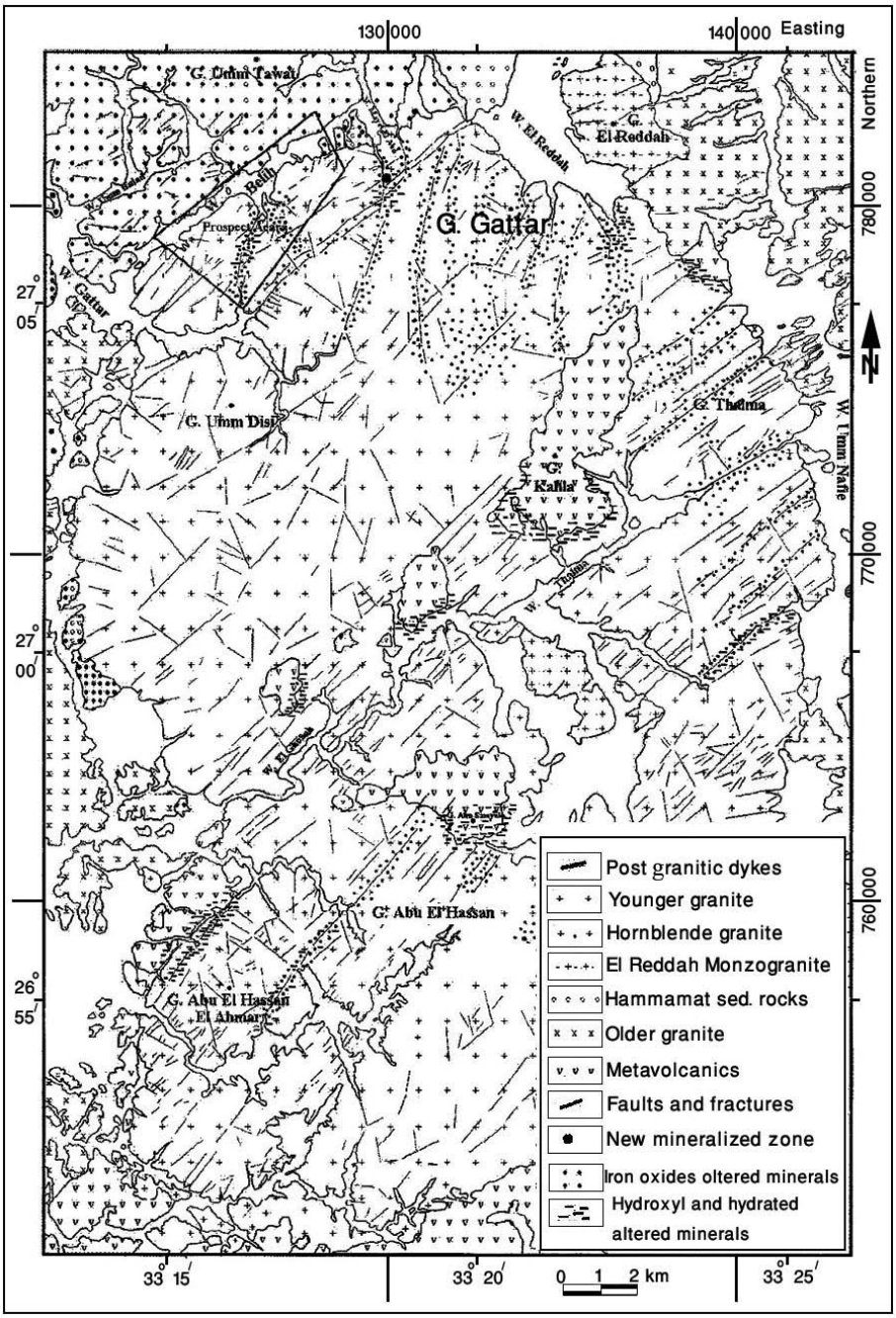

Fig. 9. Hydrothermal alteration map of Gattar pluton, interpreted from Landsat ETM images and field works.

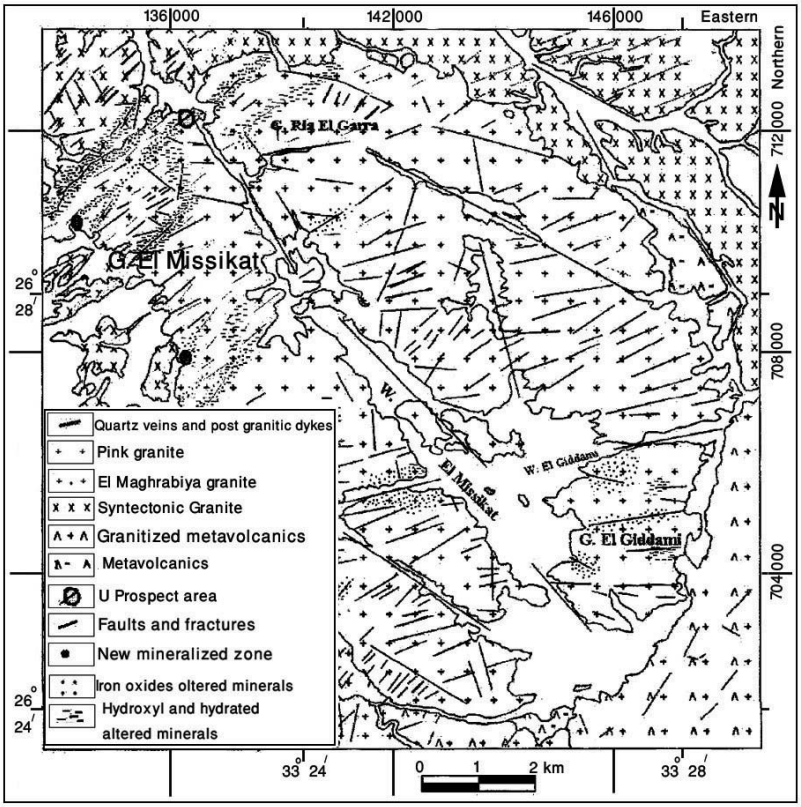

Fig. 10. Hydrothermal alteration map of El Missikat pluton, interpreted from Landsat ETM images and field works.

Two of these four newly discovered high radioactive anomalies and uranium mineralized zones are located at the western and northwestern parts of G. El Missikat granite. The third one is located at the northern part of El Erediya pluton, while the last one is found at the northern part of G. Gattar at Wadi Mayet El Abd. Table 2 shows the content of equivalent uranium, equivalent thorium and potassium for some collected samples, determined by gamma ray spectromter.

The mineralized zones of El Missikat granites are found to be mainly connected or hosted by the silicified and jasperoid veins that follow the direction of the strong and nearly vertical shear zone striking N40^{o}E-S40^{o}W in the western part of G. El Missikat, and N10^{o}E to N15^{o}E in the northwestern part. Their dips are varying from 75^{o} to 85^{o} toward the SE and ESE respectively (Fig. 12).

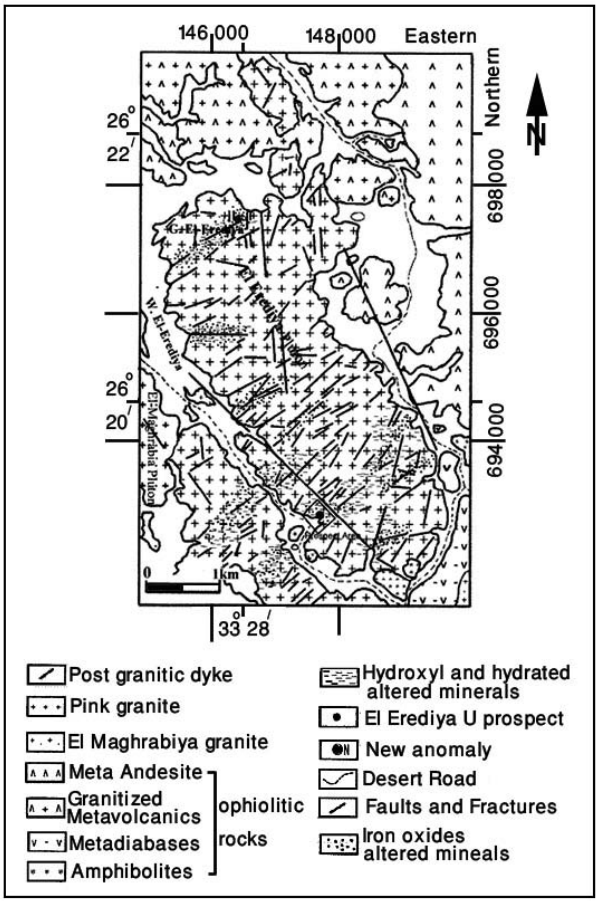

Fig. 11. Hydrothermal alteration map of El Erediya pluton, interpreted from Landsat ETM images and field works.

The radioactive anomaly at the northern part of El Erediya pluton, is mainly connected and hosted by highly altered and weathered silicified and jasperoid veins. It is structurally controlled by ENE-WSW shear zone. One of the striking features of this anomaly is its high content of equivalent thorium than equivalent uranium content. This could be attributed to the surficial leaching of large amount of uranium relative to the thorium contents, by the effect of weathering, leaving the immobile thorium as the predominant radioactive element in this area.

Along the fracture zone of Wadi Mayet El Abd at G Gattar, the mineralized part is hosted by 0.25m thickness jasperoid vein at the contact between a basic dyke and the host granite (Fig. 12). This vein is

trending N35°W-S35°E and dipping 65° to SW. The high radioactive values increase mainly near the contact between the jasperoid vein and the basic dyke. The basic dyke and the jasperoid vein are sinistrally displaced by a fault striking NNE-SSW running along the main shear zone of W. Mayet El Abd.

Fig. 12. Photographs showing:

(a) The mineralized jasperoid and silicified veins intruded west G.El Missikat granite (looking NNE).

(b) The mineralized jasperoid and silicified veins intruded northwest G.El Missikat granite (looking N).

(c) The high radioactive jasperoid veins associated with basic dyke intruding the Gattar granite,W. Mayet El Abd, looking NW.

(d) Yellow to pale yellow uranophane, separated from granite mineralized samples.

Table 2. The radioactive analysis of the selected samples collected from the high radioactive anomalies.

Location	eU ppm	eTh ppm	K %
1- West of G. El Missikat	700	4	1.24
2- Northweset of G. El Missikat	320	21	3.15
3- North of El Erediya pluton	95	181	1.35
4- W. Mayet El Abd, N.Gattar	438	18	1.02

Spectrometric, X-Ray diffraction (XRD), scanning electron microscope (SEM) and petrographic studies of the rock samples collected from the new discovery mineralized zones have been carried out to determine the mineral assemblages. The uranium minerals could be recognized only from three localities; west and northwest of G. El Missikat and in the northern part of G. Gattar at W. Mayet El Abd. The (XRD) investigation confirmed the presence of uranophane minerals $\{Ca(UO_2)_2\ (SiO_3)_2\ (OH)_2.5H_2O\}$ as uranyl silicates. This mineral is found in close association with hematite, quartz, calcite and chlorite. The ore microscopy and SEM examinations were compiled in order to identify the uranium mineral associations of the new discovered uranium mineralization. These investigations revealed the presence of uranium mineral (uranophane) as acicular needle form filling the microfractures and along the cleavage of biotite. The sulphide minerals associated with the uranium mineralization were found as relics of pyrite grains disseminated in the groundmass and filling some vugs and cavities. Pyrite is usually corroded and subjected to progressive stages of alteration in which the crystals are partially or completely altered to goethite (Fig. 12). It is worth to mention that the uranium mineralization is found adsorbed and enclose pyrite crystasls. This could indicate that the presence of pyrite created a reduced environment favorable for the precipitation and fixation of uranium.

Summary and Conclusions

This study aimed to use the capability of remote sensing techniques integrated with geological investigations to characterize the uranium bearing granites and to detect hydrothermal alteration zones, and their associated structures suitable for uranium mineralization. Two study areas including the most promising uranium bearing granites were selected; the first one represented by the area of Gattar uranium prospect, located at the northern part of the Egyptian Eastern Desert, while the second area is includes both El Missikat and El Erediya uranium

prospects, located at the central part of the Eastern Desert. The achievement of the goal of the application of remote sensing techniques on the studied granites led to identify and characterize the studied uranium bearing granites based on different remote sensing processes of ETM+ data, such as colour composite image, principal component, and colour ratio composite images.

Recognition of hydrothermal altered rocks associated with mineral deposits, was carried out using image processing technique such as band ratio images, in addition to colour ratio composite images. The spectral bands of ETM+ are well suited for recognizing assemblage of altered minerals. The hydrothermal minerals that were detected by the Landsat image processing of the data of selected areas could by classified into two groups: Hydroxyl (clay minerals) and hydrated mineral (alunite and jarosite) detected by band ratio 5/7 on one hand, and minerals containing iron (hematite and goethite) detected by band ratio 3/1 on the other hand. Applying these techniques led to recognize more than fifteen zones of altered rocks within the studied granites. The association of aplites, quartz and jasperoid veins and lamprophyric dykes and alteration processes throughout and near the mineralized sectors, appear to play an important role in the distribution and localization of the mineralization.

Image processing techniques are applied to the digital subset ETM+ data of the studied areas. These techniques generated several products of enhanced satellite imagery such as colour composite images, ratio images and principal components. These techniques have been successfully used in the lithological discrimination of uranium-bearing granites. The capabilities of remote sensing data to characterize the uranium bearing granites in addition to characterization and mapping the hydrothermal alteration zones usually help in localization of uranium mineralization. Extensive field geologic and radiometric investigations to the zones delineated by the image processing technique led to the discovery of four locations of high radioactive anomalies with some uranium mineralization, mainly connected to the studied younger granites. Two of these four newly discovered high radioactive anomalies and uranium mineralized zones are located at the western and northwestern parts of G. El Missikat granite. The third one is located at the northern part of El Erediya pluton, while the last one is found at the northern part of G.Gatter at Wadi Mayet El Abd. It is worth to mention that there are many criteria of the alteration zones that could be used as

guides for the exploration of uranium mineralization in the Egyptian younger granites. This work showed the most important criteria that are considered as tools to increase the potentiality of the uranium mineralization. Moreover, construction of the alteration maps of the different studied plutons, interpreted from the image processing helped in the discovery of new zones of mineralization, and could be used in exploration for uranium mineralization in the future.

References

Abdalla, H. M. and **El Afandy, A. H.,** (2004) Geochemistry and genesis of uranium mineralization at Missikat-Erediya area, central Eastern Desert, Egypt, *Egyptian Mineral.,* **16,** 1-33.

Abou Deif, A. (1992) The relation between the uranium mineralization and tectonics in some Pan-African granites, west of Safaga, Eastern Desert, Egypt, *Ph.D. Thesis,* Assiut Univ., Egypt, 218 p.

Attawiya, M.Y. (1990) Petrochemical and geochemical studies of granitic rocks from Gabal Gattar area, Eastern Desert, Egypt, *Arab. J. Nucl. Sci. App*., Cairo, **23**, (2) :13-30.

Bakhit, F. S. (1978) Geology and radioactive mineralization of G. El Missikat area, Eastern Desert, Egypt, *Ph.D. Thesis,* Ein Shams Univ., Cairo.

Bernstein, R. (1978) *Digital Image Processing for Remote Sensing,* Wiley, New Yourk.

Bishta, A.Z., (2004) Lithological discrimination of Gabal Gttar-Um Disi environs, North Eastern Desert of Egypt using thematic mapper data of Landsat-7, *Proc. 3rd. Int. Sympo. Geophysics, Tanta Univ*., P. 541-557.

Cuney, M. (1999) Uranium potential of Eastern Desert granites, Egypt, *Internal reports of mission from November 2 to 18*, NMA.

El Kassas, I. A. (1974) Radioactivity and geology of Wadi Atalla area, Eastern Desert of Egypt, A.R.E. *Ph.D. Thesis,* Faculty of Science, Ein Shams Univ., Cairo.

El Rakaiby, M.L. and **Shalaby, M.H.** (1992) Geology of Gabal Gattar batholith, central Eastern desert, Egypt, *Int. J. Remote Sensing*, **13**(12): 2337-2347.

El Rakaiby, M.L. (1995) The use of enhanced Landsat TM images in the characterization of uraniferous granitic rocks in the central Eastern Desert of Egypt.

El Rakaiby, M.L. (1997) remote sensing studies for dyke swarms in the central Eastern Desert of Egypt, *J. African Earth Sciences,* **24**(4): 653-656.

El Sayed, M. M.; Shalaby, M. H. and **Hassanen, M. A.** (2003) Petrological and geochemical constraints on the tectonomagmatic evolution of the late Neoproterozic granitoid suites in the Gattar area, North Eastern Desert, Egypt, *N. Jb. Miner. Abh.,* **178:** 239-275.

Greenberg, J. K. (1981) Characteristics and origin of Egyptian younger granites: Summary, *Geol. Soc. Am. Bull*., Part **II, (**92): 749-840.

Ibrahim, T. M. (2002) Geologic and radioactive studies of the besement-sedimentary contact in the area west Gabal El Missikat, Eastern Desert, Egypt, *Ph. D. Thesis,* Mansoura Univ., 215p.

Lillesand, T.M. Kiefer, R.W. and **Chipman, J.W.** (2004) *Remote Sensing and Image Interpretation*. 5th ed., John Wiley and sons Inc. New York, ISBN 0-471-25515-**7**, 763P.

Mather, P.M. (1987) *Computer Processing of Remotely Sensed Images, an Introduction,* John Wiley and Sons, ISBN: 0 – 471 – 9064 –4.

Mostafa and Bishta, A.Z. (2005) Significance of lineament patterns in rock unit classification and designation: a pilot study on the Gharib-Dara area, Northern Eastern Desert, Egypt, *Inter. J. Remote Sensing,* **26**(7): 1463-1475.

Nossair, A.A. (2005) Geological factors controlling uranium distribution and affecting its localization in G-II occurrence, Gabal Gattar, NED, Egypt, *M. SC. Thesis,* Fac. Sc., Zagazig Univ., Benha, P. 179.

PCI (1998) PCI, *GeoAnalyst, version 6.3*. PCI, Richmond Hill, Ontario, Canada.

Roz, M. E. (1994) Geology and uranium mineralization of Gebel Gatter area, North Eastern Desert, Egypt, *M.Sc.Thesis,* Al Azhar Univ., 175p.

Richards, J.A. (1995) *Remote Ssensing, Digital Image Processing, an Introduction,* Sec.Ed., Springer Velag., P. 340.

Sabins, F. F. (1999) Remote sensing for mineral exploration, *Ore Geology Reviews,* **14**: 157-183.

Sultan, M., Arvidson, R.E., and **Sturchio, N.** (1986) Mapping of serpentinites in the Eastern Desert of Egypt by using Landsat them,atic mapper data, *Geology,* **14**: 995-999.

Sultan, M., Arvidson, R.E., and **Sturchio, N.** (1987) Lithologic mapping in arid regions with Landsat thematic mapper data: Meatiq dome, Egypt, *Geological Socity of America Bulletin,* **99:** 748-762.

Vincent, R. K. (1997) *Fundamentals of Geological and Environmental Remote Sensing,* Prentice-Hall, Inc, U.S.A., 366p.

تكامل الدِراسات الجيولوجية والاستشعار عن بعد لاستكشاف تمعدنات اليورانيومِ في بعض الصخور الجرانيتية، الصحراء الشرقية، مصر

محمود هانى شلبي، وعادل زين العابدين بشته*، ومحمد السيد رز، ومحمد على الزلكي

هيئة المواد النووية، القاهرة، جمهورية مصر العربية

*و *كلية علوم الأرض، جامعة الملك عبد العزيز، جـدة، المملكة العربية السعودية*

المستخلص. تم تطبيق تقنيات الاستشعار عن بعد إلى جانب الدراسات الجيولوجية والحقلية، وذلك بغية الوصول إلى السمات المميزة للصخور الجرانيتية الحاوية لتمعدنات اليورانيوم، ومعرفة إمكانية تحديد النطاقات المتأثرة بالتغاير الحرمائي، وماهية الدور الذي تلعبه التراكيب الجيولوجية فى هذه العملية. ولقد تم اختيار منطقتين بالصحراء الشرقية بجمهورية مصر العربية ، حيث أكدت جميع الدراسات السابقة أنهما تحتويان على نسب مختلفة من تمعدنات اليورانيوم. هاتان المنطقتان هما : منطقة جبل قطار ومنطقة جبل المسيكات والعرضية. ولقد تم استخدام التقنيات الحديثة لمعالجة المرئيات الفضائية، حيث تم استخدام مرئيات لاندسات- ٧ المركبة الملونة بألوان كاذبة، وكذلك مرئيات النسبة، ومرئيات المكونات الأساسية، و تم التمييز الصخري للمنطقة. كما أعطت نتائج جيدة فى هذا العمل من أجل تمييز الجرانيتات الحاوية لليورانيوم عن غيرها من الجرانيتات الأخرى.

ونتج عن هذه الدراسات استكشاف نطاقات جديدة لتمعدنات اليورانيوم غرب وشمال غرب منطقة المسيكات، وكـذلك شـمال منطقة العرضية، وشمال جبل قطار فى وادى مية العبد. وتوصـي هذه الدراسة بضرورة تطبيق السمات المميزة للصخور الجرانيتيـة الحاوية لتمعدنات اليورانيوم المستنتجة من هـذا العمـل، وذلـك لاستكشاف مناطق جديدة ومؤهلة للتنقيب عن اليورانيوم.